

The effect of pulleys and hooks on the vibrations of cable rehabilitation robots

G. Zuccon, L. Tang, A. Doria, M. Bottin, R. Minto and G. Rosati

Abstract Cable-driven rehabilitation devices (CDRDs) represent a widespread class of rehabilitation robots used to restore individual impaired movement capabilities by performing repetitive rehabilitation training of impaired extremities. CDRDs offer several merits, such as low inertia, high payload-to-weight ratio, modularity, simple architecture, and convenient for reconfiguration. In this paper, a model that takes into account the particular features (pulleys and magnetic hook) of the cables of a CDRD is presented. Experimental tests carried out with the modal analysis approach show that the model is able to reproduce most of the dynamic properties of the vibrated system equipped with cables.

1 Introduction

Cable-driven parallel robots (also known as cable robots and CDPR) are commonly used in specific fields as industry applications [1], entertainment [2] and, especially, rehabilitation (e.g., Carex [3], CUBE [4], NereBot [5], CADEL [6, 7]). Thanks to their unique properties, such as the possibility of operating in very large workspaces, the low cost, and the high speed [8], cable robots remain a research area of great interest. The principle of operation of cable robots is based on motors, one for each cable, which pull the cables that are attached to a mass, the end effector. The combination of the action of multiple motors allow the movement of the end effector within the workspace. Compared to robotic rehabilitation devices (RRDs) with other power transmissions, CDRDs offer several advantages, such as low inertia, high payload-to-weight ratio, simple architecture, and modularity [9, 10]. Therefore, CDRDs have attracted increasing attention from researchers in the past decade [11].

G. Zuccon, A. Doria, M. Bottin, R. Minto · G. Rosati
University of Padova, Padua, Italy, e-mail: giacomo.zuccon@phd.unipd.it

L. Tang
Hunan University, Changsha, Hunan, China, e-mail: leweitang@hnu.edu.cn

The main disadvantage of cable robots relies on the cables themselves: cables are flexible and vibrate in both axial and transverse directions. The vibrations of end-effector caused by cable flexibility has been a concern for applications which require high stiffness or high accuracy [12]. To investigate the vibration of cable manipulators, during the years researchers have proposed to model cables both as linear springs [13, 14] and nonlinear springs [15], and it is common practice to model cables as axial springs [16]. As a result, transverse vibrations are neglected.

The aim of this article is to propose a vibrational analysis of a simplified cable system that reproduce the characteristics of a wire-driven rehabilitation robot, also in transverse direction. The focus is on the effects of hook mass and pulley inertia. The phenomena of cable loosening and sagging are not considered [17].

Starting from the cable system of the rehabilitation robot, in Section 2 a simplified model that evaluates the influence of the pulley inertia and the influence of the magnetic hook mass is proposed. The numerical data are reported in Section 3, while the comparison between the analytical and the experimental data is shown in Section 4. Finally, in Section 5 the modal proprieties of the cable system are discussed and future applications of the cable model are illustrated.

2 Mathematical model

The Maribot [18, 19] (Figure 1a) is a 5-DOF CDRD composed of a rigid planar structure (2-DOF) and a yielding structure moved by cables (3-DOF). The three cables are controlled by DC motors fixed to rigid links, and they support an orthosis used to hold up the patient's arm during rehabilitation exercises (Figure 1b). Cable length and orientation is determined by the presence of pulleys. To guarantee patient safety, each cable is connected to a magnetic hook near the orthosis which allows the instantaneous release of the cable when the safety-limit force is overcome.

To analyze the influence of the inertia of the cable pulleys and of the mass of the magnetic hooks on both the longitudinal and transversal vibrations, each cable is schematized by a 4-DOF model, the "simplified cable system". To simplify the dissertation, from now on, a single cable is considered.

As shown in Figure 2, the simplified cable system is composed by cable 1 ($L_1 + L_2$) which connects the motor (considered to be mechanically fixed) to the magnetic hook (mass m_2) passing through a pulley which can rotate by θ_1 . A payload equivalent to one third of the expected load on the orthosis (mass m_3) is supported by a second cable with length L_3 and it moves only vertically by y_3 due to the presence of a sliding pair.

The 4-DOF of the simplified cable system are: θ_1 , the rotation of the pulley; x_2 , the lateral displacement of the hook; y_2 and y_3 , the displacements of the two masses with respect to the configuration defined by the rigid cable.

The translation x_2 of the magnetic hook rotates L_2 by φ_2 and L_3 by φ_3 (Figure 2b). Assuming small oscillations, cables rotations are:

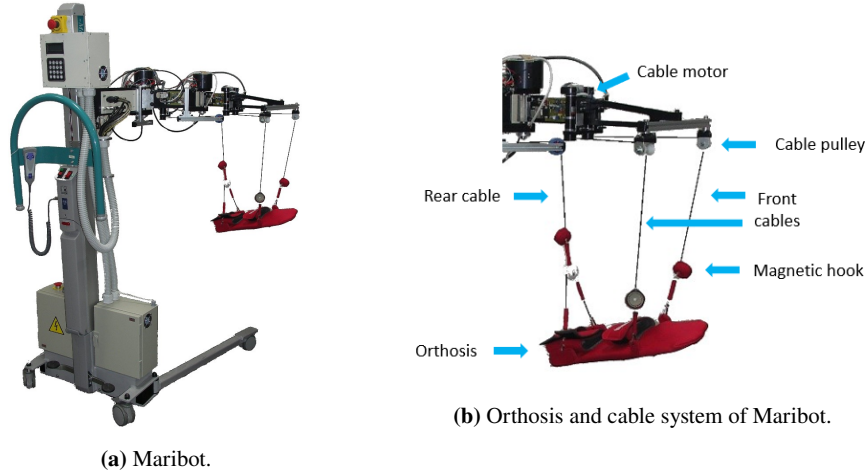


Fig. 1: Maribot rehabilitation robot.

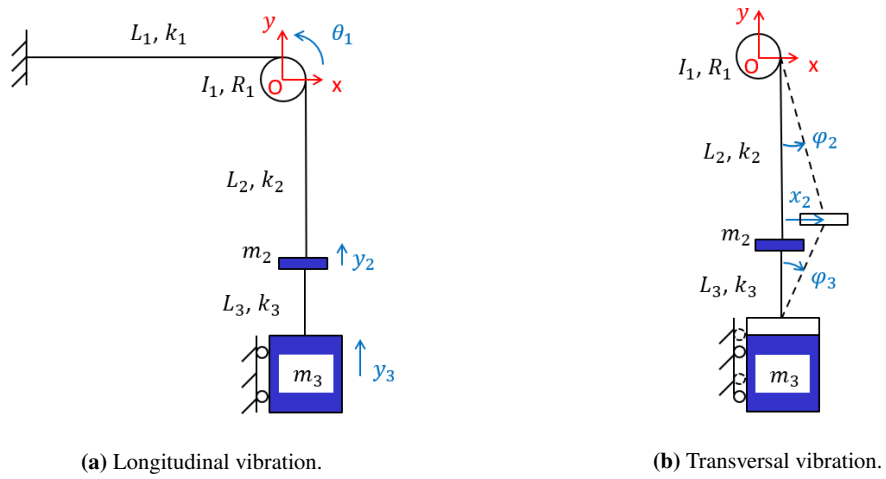


Fig. 2: Analytical model of the cable.

$$\varphi_2 = \frac{x_2}{L_2} \quad , \quad \varphi_3 = \frac{x_2}{L_3} \quad (1)$$

The vertical displacement of the masses m_2 and m_3 (h_{m2} and h_{m3} respectively) due to hook lateral displacement can be calculated as:

$$h_{m2} = L_2 - L_2 \cos(\varphi_2) \quad (2)$$

$$h_{m3} = L_2 - L_2 \cos(\varphi_2) + (L_3 - L_3 \cos(\varphi_3)) \quad (3)$$

Substituting Equation 1 in Equations 2 and 3, h_{m2} and h_{m3} become:

$$h_{m2} = \frac{1}{2} \frac{x_2^2}{L_2} \quad (4)$$

$$h_{m3} = \frac{(L_3 + L_2)x_2^2}{2L_2L_3} \quad (5)$$

These 2^{nd} order terms have a negligible effect on kinetic energy, but affect gravity potential energy.

In the hypothesis of massless cables, the system kinetic and potential energy are:

$$E_k = \frac{1}{2}I_1\dot{\theta}_1^2 + \frac{1}{2}m_2(\dot{y}_2^2 + \dot{x}_2^2) + \frac{1}{2}m_3\dot{y}_3^2 \quad (6)$$

$$E_p = \frac{1}{2}k_1(R_1\theta_1)^2 + \frac{1}{2}k_2(y_2 - R_1\theta_1)^2 + \frac{1}{2}k_3(y_3 - y_2)^2 + m_2g(h_{m2} + y_2) + m_3g(h_{m3} + y_3) \quad (7)$$

where I_1 is the pulley inertia, R_1 is the pulley radius, and k_1 , k_2 and k_3 are cables elasticity.

Using the Lagrangian approach, the equations of free undamped vibrations are:

$$\begin{bmatrix} I_1 & 0 & 0 & 0 \\ 0 & m_2 & 0 & 0 \\ 0 & 0 & m_2 & 0 \\ 0 & 0 & 0 & m_3 \end{bmatrix} \begin{Bmatrix} \ddot{\theta}_1 \\ \ddot{x}_2 \\ \ddot{y}_2 \\ \ddot{y}_3 \end{Bmatrix} + \begin{bmatrix} R_1^2(k_1 + k_2) & 0 & -R_1k_2 & 0 \\ 0 & \frac{m_2g}{L_2} + \frac{m_3g(L_2+L_3)}{L_2L_3} & 0 & 0 \\ -R_1k_2 & 0 & k_2 + k_3 & -k_3 \\ 0 & 0 & -k_3 & k_3 \end{bmatrix} \begin{Bmatrix} \theta_1 \\ x_2 \\ y_2 \\ y_3 \end{Bmatrix} = \begin{Bmatrix} 0 \\ 0 \\ 0 \\ 0 \end{Bmatrix} \quad (8)$$

Natural frequencies and modes of vibration are calculated solving the eigenvalue problem.

3 Numerical results

By means of Equation 8 and the parameters of Table 1, the influence of the inertia of the pulley I_1 and of the mass of the hook m_2 is studied, and results are shown in Table 2. The first longitudinal mode is nearly uninfluenced by both I_1 and m_2 : neglecting both of them a maximum error of 1.08% is retrieved, with a major influence of m_2 (0.98%) rather than I_1 (0.1%). As regards the transverse vibrations, Equation 8 shows that those are independent from I_1 , as confirmed by the results.

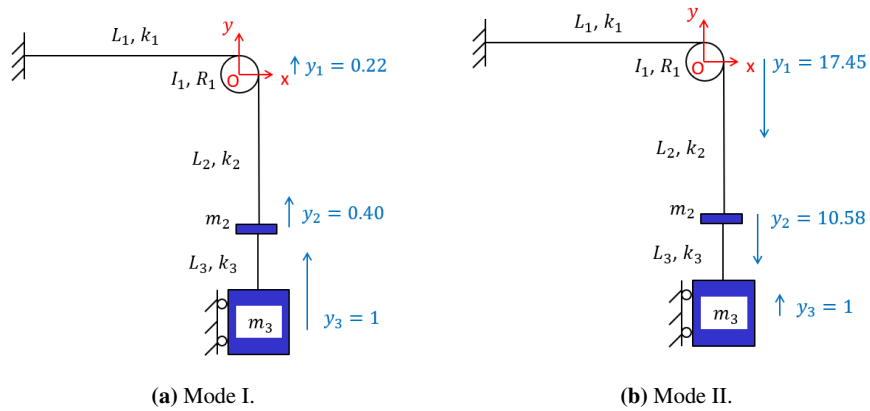
Figure 3 deals with the two longitudinal modes of vibration. In the first mode of vibration the pulley, magnetic hook and payload vibrate in phase, whereas in the second mode the pulley and hook vibrate in phase whereas the payload vibrates in phase-opposition with a small amplitude.

Table 1: Parameters of mathematical model.

Parameter	Value
$I_1 [kg \cdot m^2]$	$6.84 \cdot 10^{-6}$
$m_2 [kg]$	0.08
$m_3 [kg]$	0.596
$g [m/s^2]$	9.81
$R_1 [m]$	0.018
$L_1 [m]$	0.415
$L_2 [m]$	0.345
$L_3 [m]$	0.110
$k_1 [N/m]$	$4.245 \cdot 10^4$
$k_2 [N/m]$	$5.106 \cdot 10^4$
$k_3 [N/m]$	$1.428 \cdot 10^4$

Table 2: Numerical results of the influence of pulley inertia and magnetic hook mass on natural frequencies. All Δf_n are calculated as the difference between the baseline ($I_1 \neq 0, m_2 \neq 0$) and the case considered.

	$I_1 \neq 0, m_2 \neq 0$ f_n [Hz]	$I_1 = 0, m_2 \neq 0$ f_n [Hz]	Δf_n	$I_1 \neq 0, m_2 = 0$ f_n [Hz]	Δf_n	$I_1 = 0, m_2 = 0$ f_n [Hz]	Δf_n
Longitudinal Mode I	19.16	19.18	0.10%	19.35	0.98%	19.37	1.08%
Mode II	105.58	110.00	4.02%	253.76	58.39%	-	-
Transversal Mode I	4.79	4.79	0%	-	-	-	-

**Fig. 3:** Longitudinal modes of vibration.

4 Experimental test and validation

To experimentally validate the simplified cable system model, the test bench shown in Figure 4a was designed. During the tests a DC motor controls cable position with a

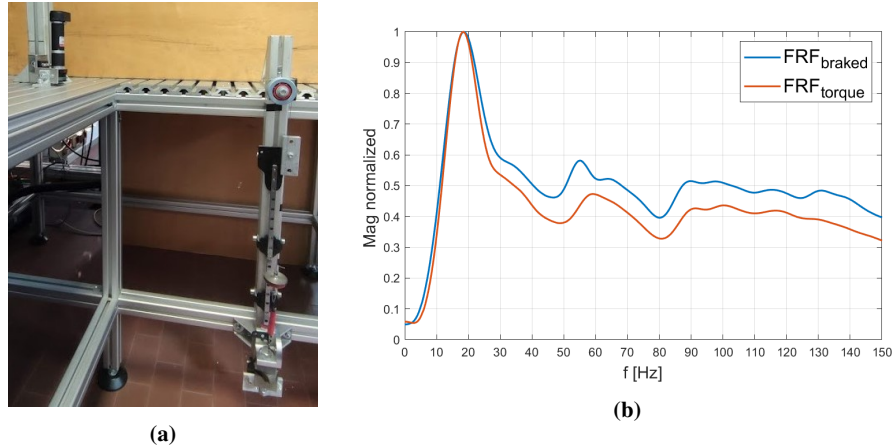


Fig. 4: Experimental test bench (a) and experimental results ($FRF_{y_3y_3}$) with torque-controlled (red) and mechanically fixed (blue) motor (b).

1/29 gearbox and a 7075T651 aluminum pulley with a diameter of $30mm$. The acetal cable pulley has a diameter of $36mm$ and is placed just above mass m_3 . The cable that goes from the motors to the hooks ($L_1 + L_2$) is a High Modulus Polyethylene (HMPE) cable ($E = 106GPa$, diameter $d = 0.46mm$) with a total length of $760mm$, whereas the cable from the hook to the payload ($L_3 = 110mm$) is in Nylon with a diameter of $1mm$.

Tests were carried out with the modal analysis approach [20] using ModalVIEW software. The acquisition system is composed of an instrumented hammer ($\pm 2.35mV/g$) with rubber tip and a monoaxial piezoelectric accelerometer ($\pm 4.56mV/g$). The sampling frequency was set at $2048Hz$ with a resolution of $0.5Hz$.

The accelerometer was positioned in sequence on the payload and on the hook. The hammer hit was excited on the payload in the vertical direction. To improve the repeatability of measurements, 7 subsequent tests carried out in the same configuration were mediated. A preliminary analysis of the natural frequencies was performed considering the motor either torque-controlled or mechanically fixed. Figure 4b shows that in both conditions the natural frequencies have a comparable value (with a deviation of less than 0.5%) hence, during the following tests, the motor was mechanically fixed.

The Frequency Response Functions (FRFs) for the longitudinal and the transversal vibrations are represented in Figure 5, normalized by the corresponding maximum value. The first index represents measurement point and direction, whereas the second index represents excitation point and direction.

Analytical and experimental results are compared in Table 3. In longitudinal direction, the experimental data is in agreement with the simplified analytical model with a deviation of 4.65% for the first mode and of 13.90% for the second mode. Fur-

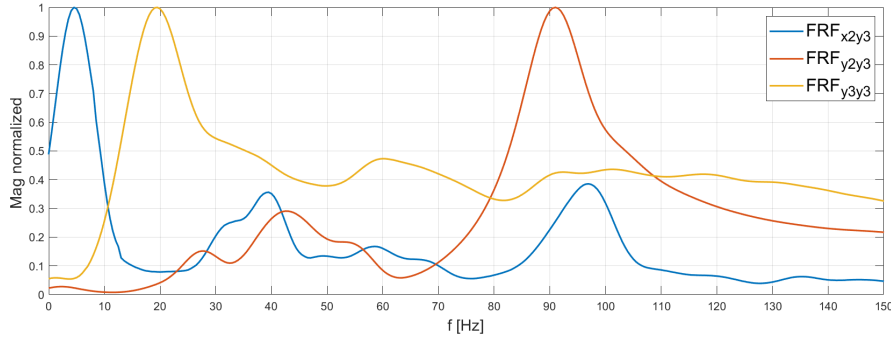


Fig. 5: Experimental FRFs. Red and yellow lines show longitudinal FRFs, while blue line shows transversal FRF.

Table 3: Comparison between analytical and experimental natural frequencies.

	Analytical f_n	Experimental f_n	Δf_n
Longitudinal Mode I [Hz]	19.37	18.47	4.65%
Longitudinal Mode II [Hz]	105.58	90.9	13.90%
Transversal Mode I [Hz]	4.79	4.41	7.93%

thermore, the transverse vibration of the magnetic hook presents a good correlation between analytical and experimental results with a deviation of 7.93%.

5 Discussion and Conclusion

The simplified cable system model made it possible to evaluate the natural frequencies and the modes of vibration of the cable robot system and the influence of the magnetic hook and the pulley on the overall dynamic behavior. The analytical model shows that the longitudinal natural frequencies do not significantly depend either on the mass of the magnetic hook or on the inertia of the pulley, as the resulting deviation is around 1%. Moreover, the inertia of the pulley does not affect the transverse natural frequencies.

These considerations were validated through experimental tests, which demonstrated the reliability of the analytical model, with deviations of 4.6% for the longitudinal natural frequencies and 7.9% for the transverse ones. Therefore, to extend the single cable vibrational model to a planar model with two cables, it is possible to simplify the system by neglecting the effects of the inertia of pulleys and of the mass of the magnetic hook in the longitudinal direction. More detailed model is under development to take into account the loosening of cables and to access the effectiveness of an innovative mechanical cable tensioning system.

References

1. Wang, Y., Yu, F., Li, Q., Chen, Y.: Configuration selection and vibration analysis of double layer suspended cable-driven parallel robot for intelligent storage system. *Lecture Notes in Computer Science (including subseries Lecture Notes in Artificial Intelligence and Lecture Notes in Bioinformatics)* **13013 LNAI**, 564–574 (2021). DOI 10.1007/978-3-030-89095-7_54
2. Chesher, C.: Robots and the moving camera in cinema, television and digital media. *Lecture Notes in Computer Science (including subseries Lecture Notes in Artificial Intelligence and Lecture Notes in Bioinformatics)* **9549**, 98–106 (2016). DOI 10.1007/978-3-319-42945-8_9
3. Mao, Y., Agrawal, S.K.: Design of a cable-driven arm exoskeleton (CAREX) for neural rehabilitation. *IEEE Transactions on Robotics* **28**(4), 922–931 (2012)
4. Cafolla, D., Russo, M., Carbone, G.: Cube, a cable-driven device for limb rehabilitation. *Journal of Bionic Engineering* **16**(3), 492–502 (2019)
5. Fanin, C., Gallina, P., Rossi, A., Zanatta, U., Masiero, S.: Nerebot: a wire-based robot for neurerehabilitation. In: *ICORR'03*, pp. 23–27 (2003). HWRS-ERC
6. Laribi, M.A., Ceccarelli, M., Sandoval, J., Bottin, M., Rosati, G.: Experimental validation of light cable-driven elbow-assisting device l-cadel design. *Journal of Bionic Engineering* (2022). DOI 10.1007/s42235-021-00133-5
7. Zuccon, G., Bottin, M., Ceccarelli, M., Rosati, G.: Design and performance of an elbow assisting mechanism. *Machines* **8**(4), 68 (2020)
8. Boschetti, G., Minto, R., Trevisani, A.: Experimental investigation of a cable robot recovery strategy. *Robotics* **10**(1), 1–18 (2021). DOI 10.3390/robotics10010035
9. Du, J., Agrawal, S.K.: Dynamic modeling of cable-driven parallel manipulators with distributed mass flexible cables. *Journal of Vibration and Acoustics* **137**(2) (2015)
10. Mayhew, D., Bachrach, B., Rymer, W.Z., Beer, R.F.: Development of the macarm-a novel cable robot for upper limb neurerehabilitation. In: *9th International Conference on Rehabilitation Robotics, 2005. ICORR 2005.*, pp. 299–302 (2005). IEEE
11. Proietti, T., Crocher, V., Roby-Brami, A., Jarrasse, N.: Upper-limb robotic exoskeletons for neurerehabilitation: a review on control strategies. *IEEE reviews in biomedical engineering* **9**, 4–14 (2016)
12. Diao, X., Ma, O.: Vibration analysis of cable-driven parallel manipulators. *Multibody system dynamics* **21**(4), 347–360 (2009)
13. Behzadipour, S., Khajepour, A.: Stiffness of cable-based parallel manipulators with application to stability analysis (2006)
14. Verhoeven, R., Hiller, M., Tadokoro, S.: Workspace, stiffness, singularities and classification of tendon-driven stewart platforms. In: *Advances in Robot Kinematics: Analysis and Control*, pp. 105–114. Springer, ??? (1998)
15. Kawamura, S., Kino, H., Won, C.: High-speed manipulation by using parallel wire-driven robots. *Robotica* **18**(1), 13–21 (2000)
16. Khosravi, M.A., Taghirad, H.D.: Dynamic analysis and control of cable driven robots with elastic cables. *Transactions of the Canadian Society for Mechanical Engineering* **35**(4), 543–557 (2011)
17. Tho, T.P., Thinh, N.T.: Analysis and evaluation of CDPR cable sagging based on ANFIS. *Mathematical Problems in Engineering* **2021** (2021)
18. Rosati, G., Andreolli, M., Biondi, A., Gallina, P.: Performance of cable suspended robots for upper limb rehabilitation. In: *2007 IEEE 10th International Conference on Rehabilitation Robotics*, pp. 385–392 (2007). IEEE
19. Rosati, G., Gallina, P., Masiero, S., Rossi, A.: Design of a new 5 dof wire-based robot for rehabilitation. In: *9th International Conference on Rehabilitation Robotics, 2005. ICORR 2005.*, pp. 430–433 (2005). IEEE
20. Doria, A., Cocuzza, S., Comand, N., Bottin, M., Rossi, A.: Analysis of the compliance properties of an industrial robot with the Mozzi axis approach. *Robotics* **8**(3), 80 (2019)